

Assessment of Effective Thermal Product of Surface Junction Thermocouples on Millisecond and Microsecond Time Scales

D. R. Buttsworth

Faculty of Engineering and Surveying

University of Southern Queensland

Toowoomba, Australia 4350

buttswod@usq.edu.au

Abstract

Surface junction thermocouples are used extensively for transient heat flux measurements, but their accuracy is dependent on the effective thermal product (TP) of the gauge and this can be a function of the time scale of interest. In the present work the response of surface junction k-type thermocouples was investigated experimentally using a water droplet calibration technique (for millisecond times scales) and a small shock tube (for microsecond time scales). Different junctions formed by scalpel blade scratches and abrasive paper were investigated. When scratches from scalpel blades were used to form the junction, the TP identified from the water droplet calibrations consistently differs by approximately 20 % depending on whether the junction was made on the chromel or alumel substrate, in accord with existing thermal properties data. However, the shock tube calibrations indicate that for scalpel-scratched junctions there is considerable variability in thermocouple response time due to effective junction depth variations produced during construction. In contrast, junctions formed with abrasive paper produced rise times consistently less than $1 \mu s$, but the water droplet and shock tube experiments both indicated significant variability in the effective TP for these gauges. The consistency in TP for scalpel-scratched junctions for millisecond time scales and the variability for junctions created with abrasive grit for both the millisecond and microsecond time scales is attributed to the differences in the effective proximity of the junction to the insulation between chromel and alumel substrates. For junctions created with abrasive grit, the effective TP is approximately 30 % smaller for microsecond time scales than it is for millisecond time scales.

1 Introduction

Surface junction thermocouples have been used extensively in the measurement of transient surface temperature and heat flux on internal combustion engine surfaces [?] and on models and probes in high speed aerodynamic facilities [?],[?]. One of the original applications for surface junction thermocouples was in the measurement of transient temperatures in gun barrels [?] and since then, various gun barrel studies have utilised similar thermocouples [?]. Surface junction thermocouples have also found application in boiling experiments [?],[?].

Surface junction thermocouples are often formed with an inner wire of either the positive or negative thermocouple material, and an outer annulus of the other thermocouple material. The wire and annulus are electrically insulated along their length, and a relatively low mass junction is formed at the exposed surface with metallic plating [?], or scratches from abrasive paper or a sharp implement [?] which causes small scale plastic deformation of the thermocouple material and bridges the insulation. Surface junction thermocouples have also been constructed using two parallel thermocouple wires [?] or ribbon elements [?] that are insulated from each other except at the exposed surface where the insulation is again bridged

by either metallic plating or small scale plastic deformation of the thermocouple material itself.

When the junction is formed by the small scale plastic deformation of the thermocouple material at the surface, the thermocouple can be successfully used for relatively fast-response measurements (rise times less than 100 μ s) in very harsh environments such as gun barrels where the erosion of surface material creates new, low thermal inertia junctions during the process [?]. Thus, in harsh flow environments surface junction thermocouples formed by small scale plastic deformation offer distinct advantages over other transient heat flux gauges such as thin film resistance gauges or calorimeters. Even in configurations where the surface thermocouple junction may be broken without being remade during the experiment, it is usually simple and inexpensive to refurbish the device using a sharp implement or some abrasive paper.

With transient heat flux gauges such as surface junction thermocouples or thin film resistance gauges which work on the principle of transient heat conduction, it is necessary to know the effective value of the gauge's thermal product (TP) - the value of $(\rho ck)^{1/2}$ for the gauge substrate. The TP is used in the derivation of the heat flux from the measured surface temperature history. Assuming the transient heat flux gauge consists of (1) a low thermal inertia temperature sensor at the substrate surface; and (2) a homogeneous semi-infinite substrate as illustrated in Fig. 1, the instantaneous (but spatially uniform) surface heat flux is related to the measured surface temperature history according to [?]:

$$q(t) = \frac{\sqrt{\rho ck}}{\sqrt{\pi}} \int_0^t \frac{dT}{d\tau} \frac{1}{\sqrt{t-\tau}} d\tau \quad (1)$$

Equation (1) indicates that the accuracy of heat flux inferred from the surface temperature history is directly dependent on the accuracy of TP, the value of $(\rho ck)^{1/2}$ for the gauge substrate.

In the case of surface junction thermocouples, calibrations are usually necessary in order to determine accurate thermal product values since at least three different materials could contribute to the effective value of TP, and the appropriate weighting for each material may be influenced by the detailed construction of each gauge and their associated junctions. Furthermore, calibrations for the effective value of TP should be performed for the time scales of interest since the semi-infinite transient thermal analysis which requires only a single value of TP (Eq. 1), is not strictly appropriate for substrates with lateral variations in thermal properties.

Gatowski et al. [?] utilized a radiative technique to identify the value of TP for various transient heat flux gauges including two different surface junction thermocouples. The general calibration process they describe requires a lamp of calibrated intensity, a value for the absorptivity of the assembled thermocouple surface (which may be coated especially for the calibration), and a relatively long exposure time (on

the order of 100 ms) to achieve useful surface temperature changes. None of these requirements are particularly restrictive except possibly the relatively long exposure time which may lead to an inappropriate value of TP if the time scales of interest are much shorter than can be assessed with this calibration technique.

Sprinks [?] proposed a fluid bath plunging technique for determining the thermal capacitance of calorimeter gauges and Jessen et al. [?] adopted a similar technique to determine the TP of their surface junction thermocouples. Fluid bath plunging calibrations require a knowledge of the thermal properties of the fluid, and measurements of both the initial bath temperature and the gauge temperature during the plunging process. Values of TP for millisecond time scales can be obtained with this fluid bath plunging technique.

In addition to a TP calibration for the time scales of interest, it is also important to confirm that the response time of the assembled thermocouple is sufficient for the required measurements since the thermocouple junctions will typically be some depth beneath the surface depending on the actual thickness of the plating or scratches that bridge the insulation. When the estimated response time based on the likely junction depth is much shorter than the required value, calibration experiments to determine the actual response time are unnecessary. However, for accurate transient heat flux measurements with a rise time on the order of 10 μ s or less, experimental confirmation of the gauge's performance (its rise time and effective value of thermal product on these time scales) will be necessary.

Surface junction thermocouple response times have been assessed using radiative heat flux techniques: Kovačs and Mesler [?] employed a flash tube discharge technique while Gatowski et al. [?] utilized a laser pulse method. However, it is difficult to determine the appropriate TP of gauges at short time scales (around 10 μ s or less) with radiative techniques due to the uncertainty in the absorptivity of the surface. Difficulties arising from absorptivity uncertainties cannot be overcome for short time scale calibrations through the application of carbon black to the surface because this additional layer thickness alters the temporal response of the gauge.

Although an influence from the insulation was identified by Kovačs and Mesler [?], previous calibration work has not clearly identified the relative importance of the various substrate materials, including the thermal property differences between the positive and negative thermocouple materials. Furthermore, previous calibration works have not identified effective TP values for microsecond time scales which may be of interest in some experiments.

The present work addresses these issues and experimentally investigates the thermal response of k-type surface junction thermocouples for millisecond and microsecond time scales with the aim of assessing and improving the accuracy of transient heat flux measurements taken with these devices. For the millisecond

time scale experiments (Section 3), a water droplet calibration technique along similar lines to the fluid bath plunging techniques of [?] and [?] is used. For the microsecond time scale experiments (Section 4), a new calibration technique using a shock tube is introduced. The shock tube method allows simultaneous assessment of both the effective TP (at microsecond time scales), and the rise time of the gauge.

2 Surface Junction Thermocouples Configuration

2.1 Design and Construction

The design of the k-type surface junction thermocouples used in the present work is illustrated in Fig. 2. The alumel annulus was machined to the required dimensions from an alumel wire (approximately 3.25 mm diameter) and a 0.8 mm diameter hole (actually made using a 5/16 inch drill) was made through its centre. The chromel wire (0.80 mm diameter) was inserted into the centre hole and the assembly was baked in a furnace at about 1000 °C for approximately 9 hours. This usually allowed sufficient time for oxidation to build up on all of the surfaces, including the region between the chromel and alumel components. However, if a finite resistance remained between the two components after this treatment, the relative positions of the components was changed and the assembly was exposed to further baking.

Once the resistance between the inner wire and the annulus exceeded 2 M Ω , and the inner wire was held firmly in position within the annulus, chromel and alumel leads were welded onto the thermocouple. The surface of the thermocouple was then treated with abrasive paper until thermocouple junctions were formed at the surface. In cases where a single scratch was used to form the thermocouple junction, the surface was polished until all of the thermocouple junctions were removed (the resistance once again exceeded 2 M Ω), and the point of a scalpel blade was drawn across the surface in the required direction and position.

2.2 Substrate Thermal Properties

According to Caldwell [?], the approximate analysis of k-type thermocouple materials is: chromel 90 % Ni, 10 % Cr; alumel 95 % Ni, 2 % Al, 2 % Mn, 1 % Si. although nickel is by far the major constituent of k-type materials, there are significant differences in the thermal properties of the chromel and alumel materials. Data collated in [?], [?], and [?] is reproduced in Figs. 3 and 4 where correlations for the specific heat and conductivity of both materials are also presented as functions of temperature. These straight-line correlations were typically obtained by identifying the slope from the data in [?] and [?] and the intercept from the manufacturer's data reported in [?]. This approach is most obvious from the

alumel specific heat correlation (Fig. 3) where the closest material composition reported in [?] (72 % Ni, 2 % Al, 25 % Mn, 1 % Si) differs significantly from the alumel analysis reported by Caldwell [?].

For chromel, the correlations are:

$$c_{cr} = 0.1786 T + 394.3, \quad (2)$$

$$k_{cr} = 0.01912 T + 12.11; \quad (3)$$

and for alumel the correlations are:

$$c_{al} = 0.07512 T + 500.8, \quad (4)$$

$$k_{al} = 0.02981 T + 18.42. \quad (5)$$

When the temperature, T is expressed in K in Eq. (2) to Eq. (5), the specific heat, c is in J/kg K and the conductivity, k is in W/m K. Based on the data reported in [?], the densities of the chromel and alumel materials are taken to be 8730 and 8600 kg/m³ respectively.

Estimates for the uncertainties in the above property values at ambient temperature are identified from the variation in values reported by different manufacturers of k-type thermocouple materials as presented in [?]. For the densities, the uncertainty is ± 1 %; for the specific heats, ± 4 %; and for the conductivities, ± 10 %. Thus, the estimated uncertainty in the value of TP for the chromel and alumel materials is ± 5.4 %. At elevated temperatures, the uncertainty in TP will be larger than this value.

Based on Eqs. (2)-(5) and the reported densities for chromel and alumel, the variation of TP with temperature for chromel and alumel materials can easily be calculated. At 20 °C, $TP_{cr} = 8313 \text{ J/m}^2 \text{ K s}^{1/2}$, and $TP_{al} = 11050 \text{ J/m}^2 \text{ K s}^{1/2}$ which amounts to a difference of $2737 \text{ J/m}^2 \text{ K s}^{1/2}$ or around 28 % which is well in excess of the estimated uncertainty in TP for these materials.

The effective value of TP for the particular thermocouple construction will depend on whether the junction is actually located on the chromel or alumel substrate materials and its proximity to the insulation, as will be demonstrated in the following sections.

3 Water Droplet Experiments

3.1 Apparatus and Methods

Water droplet calibration experiments were performed to assess the thermal product of the assembled thermocouples for millisecond time scales. The present calibration technique is similar to the fluid bath plunging technique utilised by others ([?],[?]), except that the gauge is heated and remains stationary while a drop of water at ambient temperature accelerates from rest under the action of gravity and impacts on the gauge surface. The apparatus used for the present calibrations is illustrated in Fig. 5.

When the water droplet at temperature T_w contacts the heated thermocouple at temperature T_s , there is ideally a step change in the temperature at the water-thermocouple interface. The temperature at the surface of the thermocouple, T after contact with the water is given by [?],

$$\frac{T - T_s}{T_w - T_s} = \frac{TP_w}{TP_w + TP_s} \quad (6)$$

Equation (6) strictly applies only to the hypothetical case of one-dimensional droplet impact with no rebound, and one-dimensional heat conduction with constant (temperature-independent) thermal properties in both droplet and thermocouple. Assuming the surface junction thermocouple indicates the true surface temperature T , Eq. (6) can be used to identify the value of TP_s provided the necessary temperatures are recorded, and the value of TP_w is known.

The properties of water and the thermocouple vary with temperature. However, the variations are relatively small and the experimentally observed surface temperature is approximately a step function. Thus, it is reasonable to use an effective TP value for water - TP_{we} - in Eq. (6) and the analysis will yield an effective TP value for the thermocouple.

In the present work, TP_{we} was identified from a variable thermal property finite element analysis (using a commercial software package, ANSYS 5.6). The variation in ρ , c , and k with temperature was identified using the results in [?]. A typical case where the water was initially at 22 °C with a step change in water surface temperature to 85 °C was considered in the analysis. The effective thermal product value identified from this analysis was $TP_{we} = 1643 \text{ J/m}^2 \text{ K s}^{1/2}$. Based on the comparison of a transient finite element analysis of a constant thermal property case with the analytical solution, the accuracy of the variable thermal property finite element analysis appears to be better than 0.1 %. The estimated uncertainty in TP_{we} is $\pm 2.5 \%$ which arises primarily due to the uncertainty in the thermal conductivity of water.

The gauges tested in the present work were flush mounted in a steel plate that was heated (with a hot air gun) to around 95 °C. A digital thermocouple reader indicated the surface junction temperature just before droplet impact. The surface junction thermocouple signal was amplified and then recorded throughout the droplet impact process using a digital oscilloscope. An additional plate (the insulating plate in Fig. 5) separated the heated plate from the water dropper until immediately prior to droplet release so that convective currents did not cause a significant increase in the water dropper temperature. The water droplet temperature was monitored (using the droplet thermocouple) but remained close to ambient temperature (around 22 °C) while it was forming. Heating estimates suggest that no significant increase in droplet temperature occurs during its descent towards the heated plate.

The surface junction thermocouple was aligned by eye beneath the water dropper and trial runs were performed to visually confirm the central impact of the droplets. Up to 20 runs at slightly different surface junction thermocouple temperatures were performed on any given junction. The water dropper was moved laterally a maximum distance of ± 0.5 mm relative to the visually aligned location using a traversing stage in an attempt to avoid any systematic error arising from misalignment of the water droplet and thermocouple. In a further attempt to reduce the influence of the water droplet impact dynamics, a droplet catcher consisting of a 0.2 mm thick magnetic plastic plate with a 2.2 mm diameter hole was placed directly above the thermocouple on the heated plate (see Fig. 5).

The surface junction thermocouple produced slightly different responses depending on the precise location of the droplet and the droplet catcher relative to the thermocouple junction, as is demonstrated in Fig. 6. Between run 1 (Fig. 6a) and run 2 (Fig. 6b) the droplet catcher was realigned on the plate. The principal difference between the results for these two runs is only in transient behaviour - for run 1, there is some overshoot, but for run 2, there is none. It is therefore concluded that the dynamics of the contact between the droplet and thermocouple did not have a significant influence on the mean temperature level after approximately 1 ms from droplet impact.

Some time after contact, two dimensional effects will have a significant influence on the heat transfer between the water and the thermocouple. This time is estimated to be approximately 5 ms based on the lateral distance between the thermocouple junction and water catcher (0.7 mm), and the thermal diffusivity of alumel. The measured temperatures remained steady between 1 ms and 5 ms from droplet impact as illustrated in Fig. 6.

3.2 Results

In the analysis of each run, the recorded surface junction thermocouple temperatures were normalised as illustrated in Fig. 6, and an average was taken over 200 data points (a total of 0.8 ms) centred at a

point approximately 2 ms after droplet impact. This normalised temperature step was then combined with the effective TP for water (in the manner described by Eq. (6)) to deduce the thermal properties for the thermocouple substrate, TP_s . Results from this analysis are summarised in Table 1.

For the experiments where the junction was formed by a scratch from the scalpel blade, the TP values from each run are plotted in Fig. 7. Also presented in this figure are the TP values for chromel and alumel materials at 90 °C based on the correlations reported in Section 2.2.

When the junction is formed by a scalpel scratch from the chromel substrate towards the alumel substrate, the junction is actually formed on the alumel substrate and the apparent TP corresponds closely to that of alumel identified from the correlations in Section 2.2. The mean values for the 4 data sets (series 1, 3, 5, and 9) varied between 11629 and 11090 J/m² K s^{1/2} (see Table 1) - each within the estimated ± 5.4 % uncertainty for the correlated TP value for alumel.

However, when the junction was formed by scalpel scratching towards the chromel substrate (the junction was formed on the chromel substrate), the mean values for both data sets (series 2 and 4) were 9393 and 9522 J/m² K s^{1/2} (see Table 1). Both of these values are higher than the correlated value for chromel and also slightly beyond the estimated ± 5.4 % uncertainty limits for the correlation (Section 2.2).

The derivation of TP_s from the measured data is slightly more sensitive to the temperature difference ($T_w - T_s$) than it is to the value of TP_{we} (the respective sensitivities are approximately 1.2 and 1). However, the estimated uncertainty in TP_{we} is ± 2.5 % which is significantly larger than the uncertainty in ($T_w - T_s$) which is estimated at ± 1.4 %. Thus, the estimated uncertainty in TP_s is approximately 3.9 % with the strongest contribution from the uncertainty in the TP_{we} value. This level of uncertainty may contribute to the differences in the measured and correlated chromel values presented in Fig. 7. However, other factors that need to be considered include: (1) the water used in the experiments was distilled, but the level and characteristics of probable contaminants was not identified; and (2) although the junction is made on the chromel substrate, the gauge is actually composed of 3 different materials and the 1 ms time scale is sufficient for each of these to contribute to the effective thermal product value of the substrate.

The difference between the effective thermal product values for the junctions formed by scalpel scratching onto chromel and alumel substrates remains significant and is consistent for all of the scalpel scratched junctions tested. This result suggests that it may not be necessary to calibrate each surface junction thermocouple to determine TP_s provided the response time for the scratched junction is adequate. Based on the present calibration data, if a scalpel scratch (of the type described) is used to make a junction on the alumel substrate, it is anticipated that $TP_s = 11386$ J/m² K s^{1/2} and if it is formed on the chromel substrate $TP_s = 9458$ J/m² K s^{1/2} with 95 % confidence limits of ± 3.1 % (based on (twice) the standard

deviation of the mean values for the scalpel scratched junctions in Table 1.)

The situation is somewhat different when the thermocouple junctions are created using abrasive paper. For series 7 experiments, multiple junctions were created by carefully drawing a small area of 400 grit abrasive paper from the chromel substrate onto the alumel substrate and all the localised junctions were created on the alumel substrate. However, the value of $TP_s = 9494 \text{ J/m}^2 \text{ K s}^{1/2}$ is significantly lower than the correlated value for alumel. With the 400 grit scratches, which are much finer than those created with a scalpel blade, the effective locations of the thermocouple junctions are much closer to the insulation than when the scalpel is used to create the junctions. It appears probable that the thermal properties of the insulation have a stronger influence on the effective values of the TP when fine junctions are created with abrasive grit.

When junctions are created with abrasive grit and a relatively large area of abrasive paper is drawn across the entire face of the thermocouple (as in series 6 and 8), junctions are likely to be created on both the chromel and alumel substrates. The number of junctions on each substrate of the thermocouple may not be equal so it is possible that the TP of one of the substrate materials may dominate. As well, there is also the probable influence of the insulation thermal properties. Thus, significant variations in the effective thermal product are observed for junctions created using abrasive grit (Fig. 8).

4 Shock Tube Experiments

4.1 Apparatus and Methods

To identify the response of the surface junction thermocouples on a much shorter time scale than could be achieved with the water droplet experiments, calibration experiments were performed in a small shock tube. The shock tube used in the present work had an overall length of approximately 2.2 m and is illustrated in Fig. 9.

Prior to a shock tube experiment, ambient air from the laboratory environment (at a temperature of 21.6 °C and absolute pressure of 94.3 kPa) filled both the shock tube and driver sections. The shock tube and driver sections were isolated from each other with a number of cellophane diaphragms (usually between 4 and 6). The driver section was then filled with helium until the diaphragms ruptured.

Two piezoelectric pressure transducers and 5 surface junction thermocouples were mounted flush with the inside wall of the shock tube. Signals from the pressure transducers and the tube thermocouples were used to identify the propagation of the shock wave along the shock tube. Signals from the pressure transducers and all of the thermocouples (including those being calibrated) were recorded using digital oscilloscopes

at a rate of 5 MSamples/s. A linear regression was used to determine the shock speed from the shock timing data. Shock speeds of between 510 and 627 m/s were established for the present calibration experiments (see Table 2). The uncertainty estimate for the shock speed based on the regression analysis and the shock timing data is $\pm 0.7\%$.

When the shock wave reflects off the end wall of the shock tube, the air in contact with the end wall experiences a step change in temperature (assuming idealised one dimensional gas dynamic and heat transfer processes with constant thermal properties). A calibration technique very similar to that adopted in the water droplet calibration experiments is therefore possible.

Thermocouples were flush mounted in the shock tube end wall. The magnitude of the step indicated by the thermocouples will ideally be given by [?],

$$\frac{T - T_s}{T_a - T_s} = \frac{TP_a}{TP_a + TP_s} \quad (7)$$

provided the thermocouple truly measures the temperature at the interface between the air and the substrate. In contrast to the water droplet experiments, it is possible to simplify this result for the shock tube experiments to,

$$\frac{T - T_s}{T_a - T_s} \approx \frac{TP_a}{TP_s} \quad (8)$$

with a typical error of less than 0.2 % since $TP_a \ll TP_s$. Provided the thermocouple temperature is recorded during the shock reflection process and the temperature step in the air due to shock compression ($T_a - T_s$) and the TP_a) can be determined with sufficient precision, Eq. (8) can be used to derive the effective value of TP_s for microsecond time scales.

The air temperature change ($T_a - T_s$) reported in Table 2 was calculated from the incident shock speed (u) using a calorically imperfect, ideal gas analysis for air. The constant pressure specific heat and enthalpy of air were calculated using the correlation presented in [?]. The thermal conductivity of air (used in the calculation of TP_a) was estimated using Sutherland's law [?].

The temperature difference between the air at the thermocouple interface and the air at locations unaffected by the heat conduction, varied between 191 and 341 K for the range of conditions used in the experiments (Table 2). For such temperature differences, the relevant properties of air (ρ , c , and k) vary significantly. To determine an effective value of TP_a under such conditions, variable thermal property transient heat conduction calculations were performed using a commercial finite element program (ANSYS 5.6). For ρ , the variation with temperature was calculated from the ideal gas equation; for c , the

variation was again determined from the correlation in [?]; and for k , Sutherland's law [?] was again used. From these finite element calculations, effective values for the shock compressed air's TP were determined for each run - as indicated in the last column in Table 2. The accuracy of these variable property finite element calculations is estimated to be around 0.35 % based on the difference between a constant property finite element solution (with the same level of discretisation as the variable property solutions) and the analytical solution. The effective thermal product for air TP_{ae} in Table 2 was used in the place of TP_a in Eq. (8) for the analysis of the results.

4.2 Results

A number of thermocouples with different forms of scratched junction were tested. Experiments were performed with thermocouples located on the shock tube axis and off-axis a maximum radial distance of 4.5 mm. Table 3 summarises the configurations and results from the shock tube experiments.

An example of the output produced by the surface junction thermocouples is presented in Fig. 10. Because the thermal product of the air is small relative to that of the thermocouple, very small surface temperature changes were obtained (only 0.9 K for the Fig. 10 experiment) even though there was a large change in the air temperature (341 K for the Fig. 10 experiment) due to shock compression.

The air in contact with the surface junction thermocouple remains stationary for only a short period of time following shock reflection. This is because two dimensional effects (eg, boundary layer jetting) will disturb the air at the end wall. The useful test period for the present analysis is estimated using the time taken for a sonic disturbance from the corner region (where the end wall meets the shock tube wall) to reach the thermocouple location. Using this approach, the available test time will be shortest (in run 8) when the sonic speed behind the reflected shock is highest (approximately 500 m/s) and the surface junction thermocouple is furthest from the shock tube axis (giving a distance between the corner and the thermocouple of approximately 9 mm). In this case, the estimated useful test time from shock reflection is approximately 18 μ s.

The results in Fig. 10 indicate that a small change in level (around 5 %) has occurred by 18 μ s after shock reflection so a more conservative approach was adopted in the analysis of the present results. To identify the step in the surface temperature for each result, the recorded signal was averaged over the period from 1 to 10 μ s after shock reflection. Examples of signals obtained during the time period to 10 μ s from shock reflection are given in a normalised form in Fig. 11. Temperature step values prior to normalisation but averaged from 1 to 10 μ s are presented (as $T - T_s$) in Table 3 for each of the reported surface junction thermocouple experiments.

The values of $(T - T_s)TP_r / (T_a - T_s)TP_{ae}$ reported in Table 3 are inversely proportional to the value of TP_s scaled by a factor of 10000 (which is the thermal product reference value, TP_r). The repeatability of the shock tube calibration technique is assessed using data from runs 2 to 5 which are essentially repeated experiments with the same configuration. Considering the data from gauge 1, these runs produced a mean value of $TP_s = 4769 \text{ J/m}^2 \text{ K s}^{1/2}$ with a standard deviation of 4.6 %. This level of variability is significantly higher than uncertainty estimates for the present analysis which indicate that the strongest contributions to the calculated values of $(T_a - T_s)TP_{ae}$ are from the measured shock speed (sensitivity of 4.43, and uncertainty of ± 0.7 %) and thermal conductivity of air (sensitivity of 0.5, and uncertainty of ± 2 %), yielding a total uncertainty of around ± 3.3 %.

It may be possible to explain the high run-to-run variability ($2\sigma = 9.2$ %) relative to the estimated uncertainty (± 3.3 %) in terms of the cleaning treatment the gauges received between each shock tube run. Fragments of the cellophane diaphragms were removed from the shock tube end wall after each experiment by rubbing the end wall with a cloth. However, some diaphragm material may have remained, and some small changes in the junction structure may have occurred. Another contribution may arise from a distortion of the incident shock front or different shock reflection processes due to variations in the shock impact angle (which is nominally normal).

For runs 2 to 5, gauge 2 appeared to have a poor rise time (at least $10 \mu\text{s}$) in comparison with gauge 1 (which had a rise time of less than $1 \mu\text{s}$). Thus, the signal-to-noise ratio for gauge 2 is poor, the apparent value of TP_s for gauge 2 is much larger, and there is greater variation in TP_s for gauge 2 over these runs (2 to 5), relative to that for gauge 1 (see Table 3).

The rise time for gauges with junctions formed using 400 or 1200 grit abrasive paper was typically less than $1 \mu\text{s}$ (eg, Fig. 11a and 11b). However, when 120 grit was used, a rise time of approximately $1 \mu\text{s}$ was registered (Fig. 11c). Values of TP_s for junctions created with abrasive grit varied between 5824 and 7119 $\text{J/m}^2 \text{ K s}^{1/2}$ with a mean of $6704 \text{ J/m}^2 \text{ K s}^{1/2}$ and a standard deviation of 9.0 %. This level of variation is greater than can be expected based on the observed run-to-run variability (standard deviation of 4.6 %).

5 Discussion

For junctions created using abrasive grit, the values of TP_s identified from the shock tube calibrations were on average 30 % lower than the values obtained in the water droplet calibrations. The lower values of TP_s at the shorter time scales can be attributed to the proximity of the thermocouple junction to the insulating material. This conclusion is supported by the work of Kovács and Mesler [?] although

they express their results in terms of the deviation of a measured surface temperature history from the anticipated form.

Kovács and Mesler [?] demonstrated that when a thin layer of material (in the form of either a scratch or a deposited layer) bridges the insulation, the measured temperature signal would ‘overshoot’ the anticipated surface temperature history (based on a single TP_s value). In such cases they claim that, “the junction becomes, to a degree, thermally insulated from the bulk material of the slab” and thus “cannot transmit this heat as fast as the other surface layers that are backed up by a heat conducting solid”. However, the thermocouple junctions are actually located on the chromel and/or alumel substrates, not immediately above the insulation material. Thus, the true reason for the so-called overshoot phenomena is most likely the proximity of the location of the junction to the insulation layer. With decreases in the thickness of the layers bridging the insulating material, the effective junction location will move closer to the insulation and the thermal properties of the insulation will play a more significant role in determining the effective value of TP_s for the gauge, particularly for the higher frequency components of the heat flux.

Both the water droplet and shock tube experiments demonstrated that there is significant variability in the values of TP_s for junctions created using abrasive grit on both millisecond and microsecond time scales. For the abrasive grit junctions tested in the water droplet experiments, the standard deviation of the mean values of TP_s was 6.7 %, and for the shock tube experiments the standard deviation was 9.0 %. When abrasive paper is drawn across the entire face of the thermocouple, many junctions are usually created with the abrasive grit and it is difficult to quantify the number of junctions on each of the chromel and alumel substrates. Thus, the differing thermal properties of the chromel and alumel substrate materials coupled with the uncertain weighting for each may contribute to the variability. However, in the water droplet experiments, localised unidirectional abrasive grit junctions were also tested and also exhibited significant variability. Thus, for junctions created with abrasive grit, it appears likely that differences in the proximity of the junction to the insulation due to construction variability contribute to the observed variations in TP_s .

In contrast, junctions created using a scalpel blade produce consistent values of TP_s for millisecond times scales (from the water droplet experiments), principally because the effective junction location is a relatively long way from the insulation. Microscopic examination indicates that the junctions extend a maximum distance of around 30 μm from the insulation. The magnitude of TP_s identified from the water droplet experiments depends on whether the junction is actually located on the chromel or alumel substrates, and is reasonably consistent with predictions based on correlations for previously reported thermal property data.

The shock tube experiments revealed that for microsecond times scales, the junctions created with scalpel scratches produced inconsistent results. In one case, the apparent rise time was less than 1 μs whereas

the other case produced a rise time estimated to be in excess of $10 \mu\text{s}$. These junctions were created by hand and there was probably considerable variability in the effective depth of the junction which has a direct impact on the rise time of the gauge. For junctions created with abrasive paper, the rise time was consistently less than $1 \mu\text{s}$ when 400 and 1200 grit was used. In the case where 120 grit was used, the rise time appeared to be approximately $1 \mu\text{s}$.

6 Practical Significance

The results of the present work have significant implications for the design of transient heat conduction experiments using surface junction thermocouples, and associated calibration requirements for such devices. If the effective junction location is sufficiently far from the insulation, the effective thermal product (TP) of the thermocouple approaches that of the substrate on which the junction is made. For example, a single scalpel scratch bridging the insulation by starting on the chromel and finishing on the alumel produced a junction on the alumel substrate at an average location of approximately $15 \mu\text{m}$ from the insulation. This distance was sufficient for the observed TP to consistently coincide with that of alumel (as reported in the existing literature) for millisecond time scales. Thus, in transient heat flux experiments where millisecond time scales are of interest (eg, mean heat flux levels in some shock tunnel facilities) many scalpel scratched gauges might be constructed and used, but only a few samples need be calibrated to identify the appropriate TP for all of the gauges. In transient heat flux experiments where microsecond time scales are of interest, junctions created with abrasive grit are more likely to produce the required rise times. However, for junctions created with abrasive grit there is much more variability in the TP, and calibrations for each gauge and associated junction construction are likely to be needed if transient heat flux data to a precision of better than $\pm 20 \%$ is required.

7 Conclusion

The present work uses a water droplet calibration technique to identify the effective thermal product (TP) of various surface junctions for millisecond time scales. Using this water droplet technique it has been possible to identify differences in the TP of the chromel and alumel substrates in an assembled k-type surface junction thermocouple. The present work also introduces a new shock tube calibration technique in order to study the response of surface junction thermocouples (in terms of their effective TP and rise time) for microsecond time scales.

Junctions created with single scalpel scratches are located near the surface of either the chromel or alumel substrates, depending on the direction of the scratch. The water droplet calibration data demonstrates

that there are significant differences between the TP for junctions formed on the chromel substrate and those formed on the alumel substrate. From an examination of the existing data for chromel and alumel materials, the TP of alumel is expected to be approximately 28 % larger than that of chromel at approximately room temperature. The scalpel scratches tested in the water droplet experiments produced consistent thermal product values (to within ± 3.1 %) that are in general agreement with existing thermal properties information for time millisecond time scales. However, for scalpel scratched junctions and microsecond time scales (obtained in the shock tube experiments), inconsistent results were obtained principally because of the variability in the effective junction depth which has a direct influence on the rise time of the gauges.

When abrasive paper was used to create the junctions, the rise time of the gauges observed in the shock tube experiments was consistently less than $1 \mu\text{s}$. However, there was considerable variability in the magnitude of the effective TP identified in both the shock tube experiments and the water droplet experiments. In general however, the TP for the microsecond time scales (from the shock tube experiments) was approximately 30 % lower than the value identified for the millisecond time scales (from the water droplet experiments). The variability in thermal product is attributed to the influence of the insulation between the two substrates. The insulation is likely to have a more significant influence for junctions created with abrasive grit than for scalpel scratched junctions because the effective junction location will be much closer to the insulation in the abrasive grit case because the physical scale of the plastic deformation is much finer when abrasive grit is used.

8 Future Research

Although the shock tube technique introduced in the present work allows the investigation of surface junction thermocouple response for microsecond time scales, it may not be applicable to in-situ calibration of gauges. However, the water droplet calibration technique could offer an elegant calibration solution for millisecond time scales and configurations where a fluid bath plunging technique and shock tube calibration are not possible. Thus, if transient heat flux data with a precision of better than ± 20 % for microsecond time scales is to be obtained using surface junction thermocouples, it will be necessary to correlate the effective thermal product for microsecond time scales with the effective value for millisecond time scales. Such a correlation cannot be identified with the present data (except to say that on average, the thermal product on microsecond time scales is approximately 30 % lower than it is for millisecond time scales) because different junctions were tested in the shock tube and water droplet experiments. However, the identification of a more precise correlation would be possible if the same sample gauges and associated junctions are calibrated with both the water droplet and shock tube techniques as described in the present work.

Acknowledgement

The author wishes to acknowledge the Australian Research Council for the provision of a Small Grant which supported this work. Mr Brian Aston from the Faculty's Mechanical Workshop is also thanked for his assistance in the construction of the thermocouples.

Nomenclature

c	specific heat at constant pressure (J/kg K)
k	thermal conductivity (W/m K)
q	surface heat flux (W/m ²)
t	time from start of heating or cooling (s)
T	temperature at the surface, temperature measured by the thermocouple (°C or K)
T_s	temperature of thermocouple substrate at locations unaffected by transient conduction (°C or K)
T_a	temperature of air at locations unaffected by transient conduction (°C or K)
T_w	temperature of water at locations unaffected by transient conduction (°C or K)
TP	thermal product, $(\rho ck)^{1/2}$ (J/m ² K s ^{1/2})
TP _r	thermal product reference value, $(\rho ck)_r^{1/2} = 10000$ (J/m ² K s ^{1/2})
u	shock speed (m/s)
x	distance from surface of substrate (m)
α	thermal diffusivity, $k/\rho c$ (m ² /s)
ρ	density (kg/m ³)
σ	standard deviation (%)
τ	dummy variable for integration wrt time (s)
subscripts	
a	air
al	alumel
cr	chromel
e	effective value based on a variable thermal property analysis
r	reference value
s	thermocouple substrate
w	water

series	gauge no.	insulation thickness (μm)	scratch description	no. of runs	TP_s ($\text{J}/\text{m}^2 \text{ K s}^{1/2}$)	σ (%)
1	1	10 (estimated)	scalpel scratch 60 μm wide, alumel junction	20	11433	1.8
2	1	10	scalpel scratch 60 μm wide, chromel junction	20	9393	2.6
3	1	25	scalpel scratch 80 μm wide, alumel junction	20	11629	1.7
4	1	25	scalpel scratch 70 μm wide, chromel junction	20	9522	2.1
5	1	10	scalpel scratch 70 μm wide, alumel junction	20	11090	2.2
6	3	10	400 grit paper, chromel and alumel junctions	20	10107	0.9
7	3	10	400 grit paper, alumel junctions	10	9494	1.2
8	4	10 to 30	120 grit paper, chromel and alumel junctions	20	8735	1.7
9	4	15 (estimated)	scalpel scratch, alumel junction	10	11393	4.3
10	3	10	400 grit paper, chromel junctions	10	10079	2.5

Table 1: Summary of the water droplet calibration experiments.

run	u	$T_a - T_s$	TP_a	TP_{ae}
no.	(m/s)	(K)	(J/m ² K s ^{1/2})	(J/m ² K s ^{1/2})
1	510	191	11.91	11.44
2	523	207	12.46	11.93
3	610	318	16.25	15.31
4	590	290	15.30	14.50
5	591	293	15.42	14.58
6	582	282	15.05	14.24
7	592	294	15.44	14.61
8	627	341	16.99	15.99
9	585	284	15.11	14.32

Table 2: Summary of the conditions produced in the shock tube experiments.

run no.	gauge no.	radial		$T - T_s$ (K)	$\frac{(T-T_s)TP_r}{(T_a-T_s)TP_{ae}}$	σ (%)	TP_s $J/m^2 K s^{1/2}$
		location (mm)	scratch description				
1	1	0	400 grit paper	0.317	1.451	31	6892
	2	4.5	400 grit paper	0.353	1.615	29	6192
2	1	0	alumel junction	0.485	1.967	26	5083
	2	4.5	chromel junction	0.228	0.924	61	10828
3	1	0	alumel junction	1.052	2.160	13	4630
	2	4.5	chromel junction	0.422	0.867	42	11530
4	1	0	alumel junction	0.914	2.172	13	4604
	2	4.5	chromel junction	0.290	0.690	52	14500
5	1	0	alumel junction	0.898	2.102	14	4757
	2	4.5	chromel junction	0.559	1.308	19	7646
6	1	0	400 grit paper	0.569	1.418	24	7055
	2	4.5	400 grit paper	0.563	1.405	22	7119
7	5	4.5	1200 grit paper	0.735	1.710	14	5847
8	5	4.5	400 grit paper	0.936	1.717	13	5824
9	5	4.5	120 grit paper	0.577	1.418	20	7053

Table 3: Summary of the results from the shock tube calibration experiments.

List of Figures

1	Illustration of transient conduction principle.	23
2	Illustration of the present k-type surface junction thermocouples.	24
3	Variation of chromel and alumel specific heat with temperature.	25
4	Variation of chromel and alumel conductivity with temperature.	26
5	Illustration of the apparatus used in the water droplet calibration experiments.	27
6	Example of normalised responses obtained in water droplet calibration experiments.	27
7	Results from water droplet calibration experiments for junctions created with a scalpel blade.	28
8	Results from water droplet calibration experiments for junctions created with abrasive paper.	29
9	Illustration of the configuration used in the shock tube calibration experiments.	30
10	Example of the thermocouple temperature measured in the shock tube calibration experiments.	30
11	Results from shock tube calibration experiments: runs 7, 8, and 9 (junctions created using abrasive paper).	31

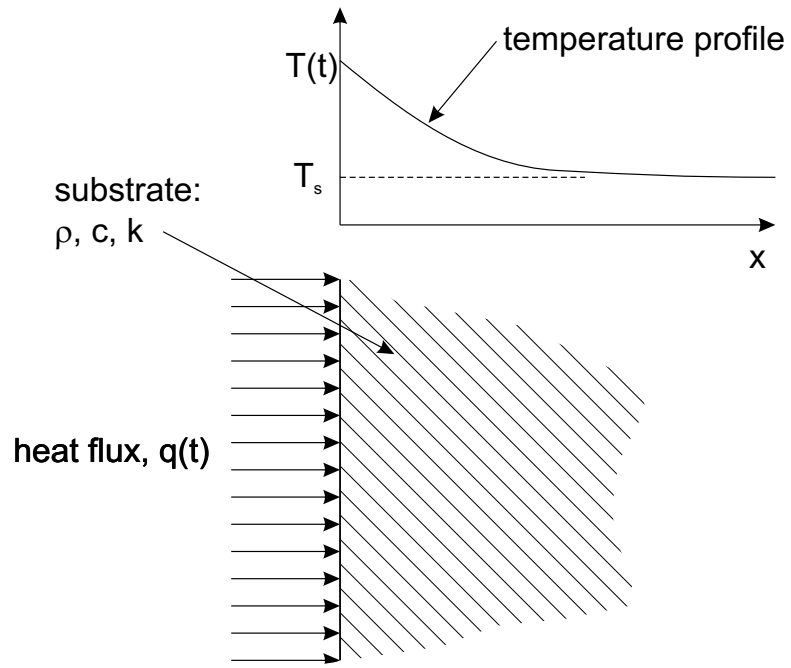


Figure 1: Illustration of transient conduction principle.

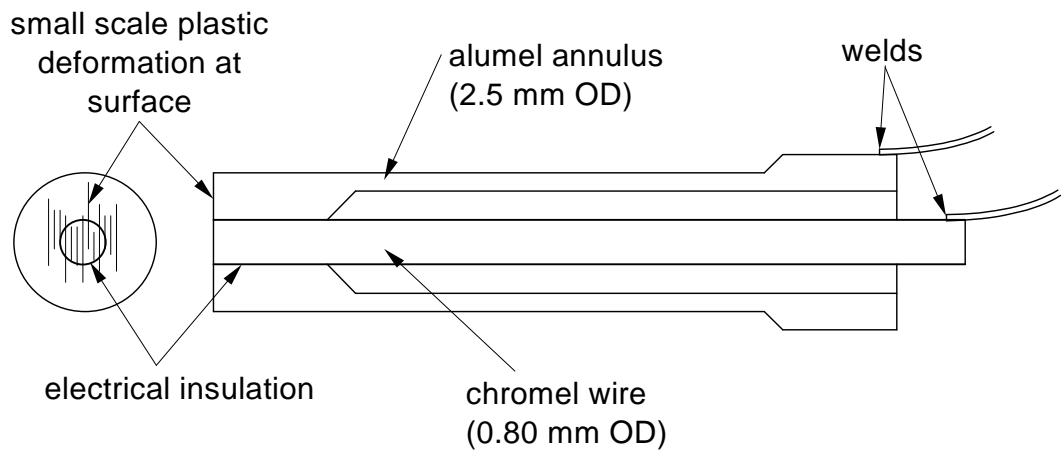


Figure 2: Illustration of the present k-type surface junction thermocouples.

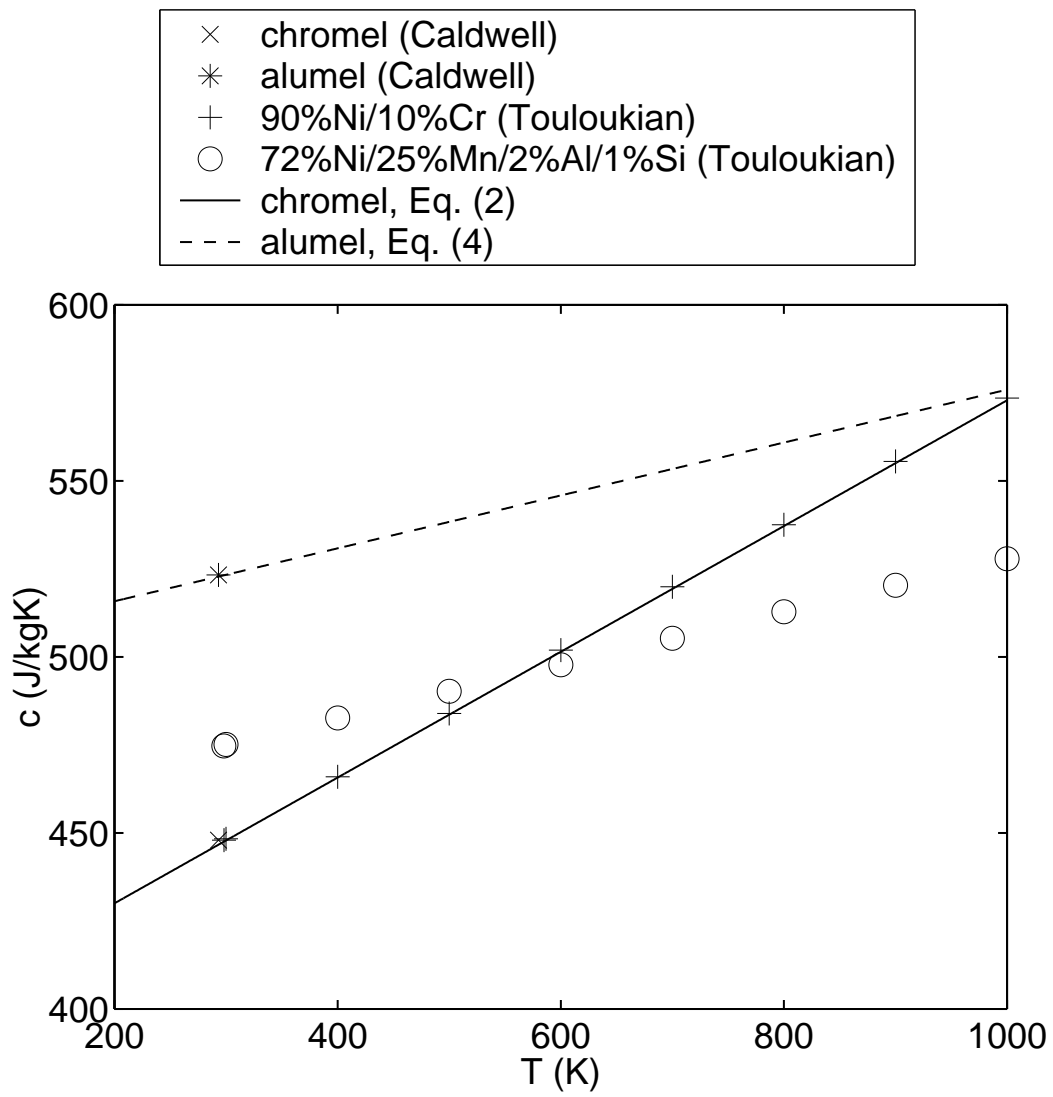


Figure 3: Variation of chromel and alumel specific heat with temperature.

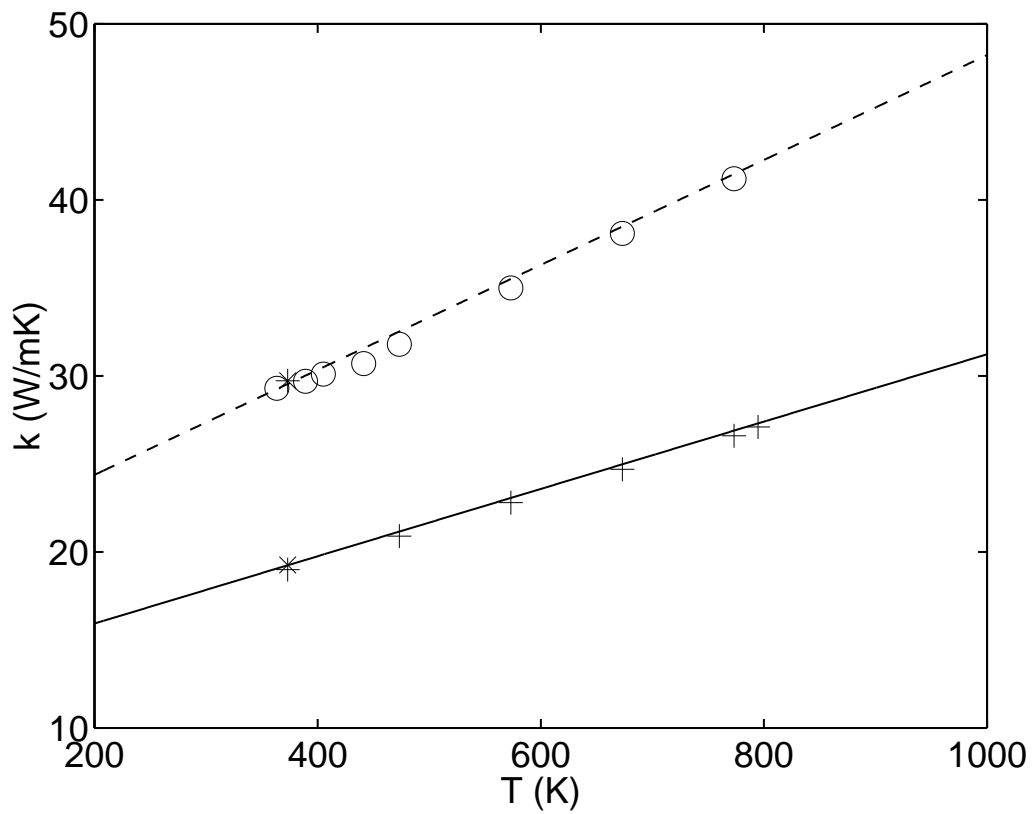
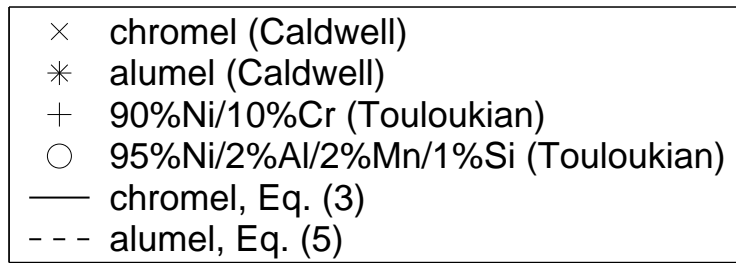


Figure 4: Variation of chromel and alumel conductivity with temperature.

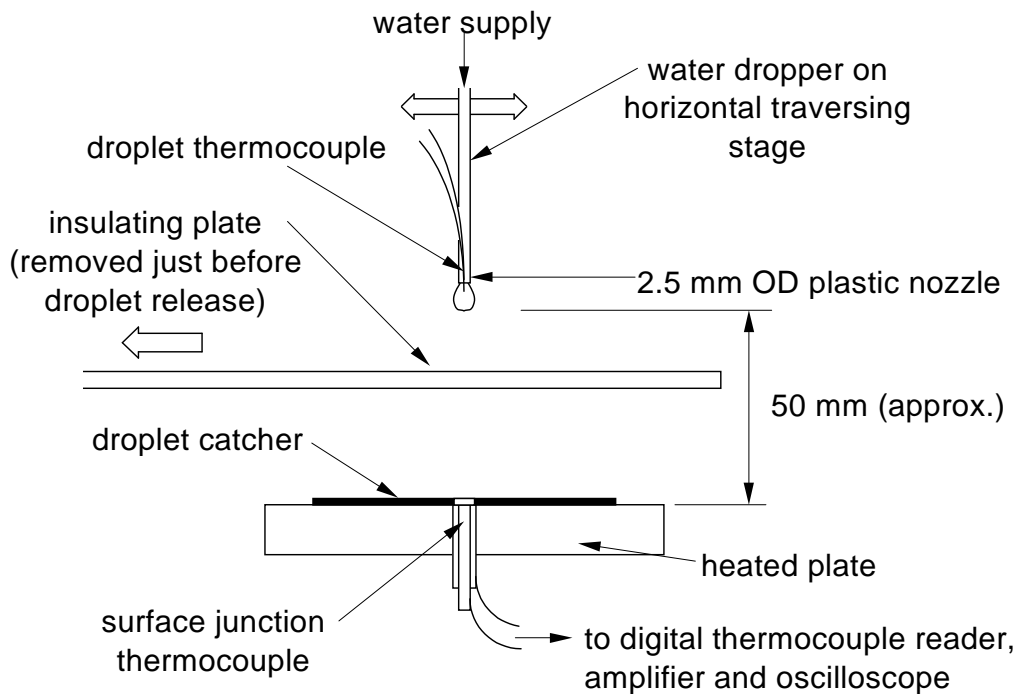


Figure 5: Illustration of the apparatus used in the water droplet calibration experiments.

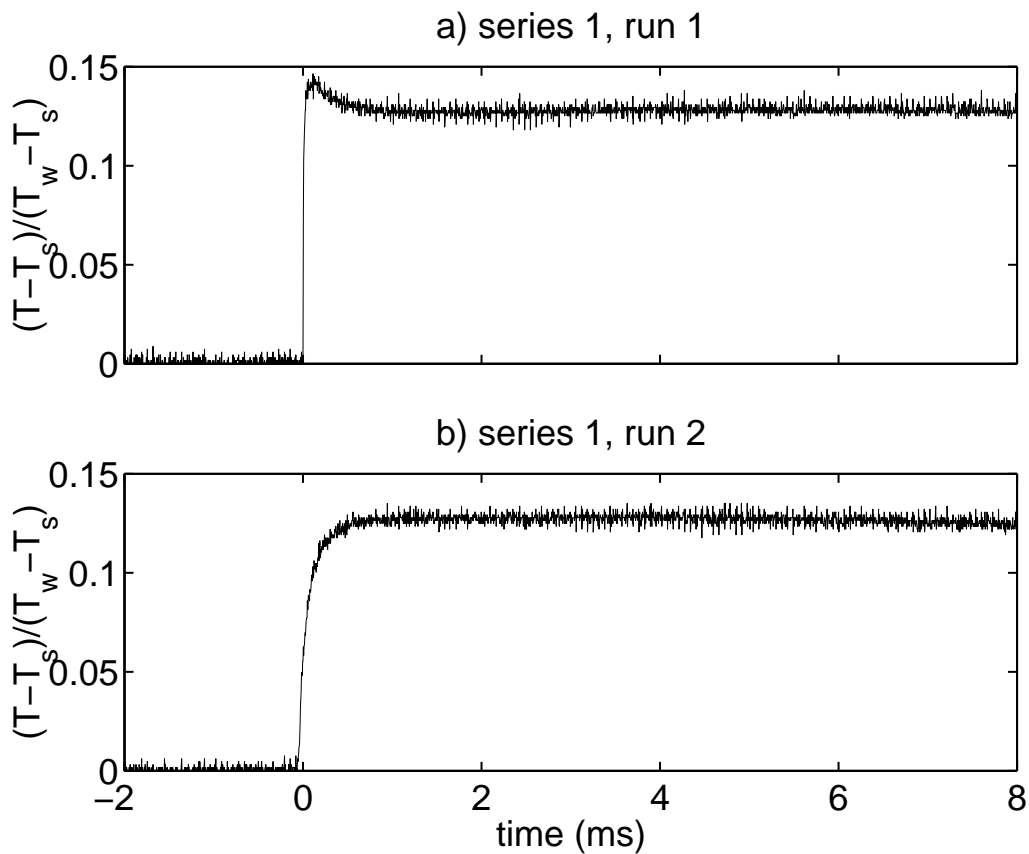


Figure 6: Example of normalised responses obtained in water droplet calibration experiments.

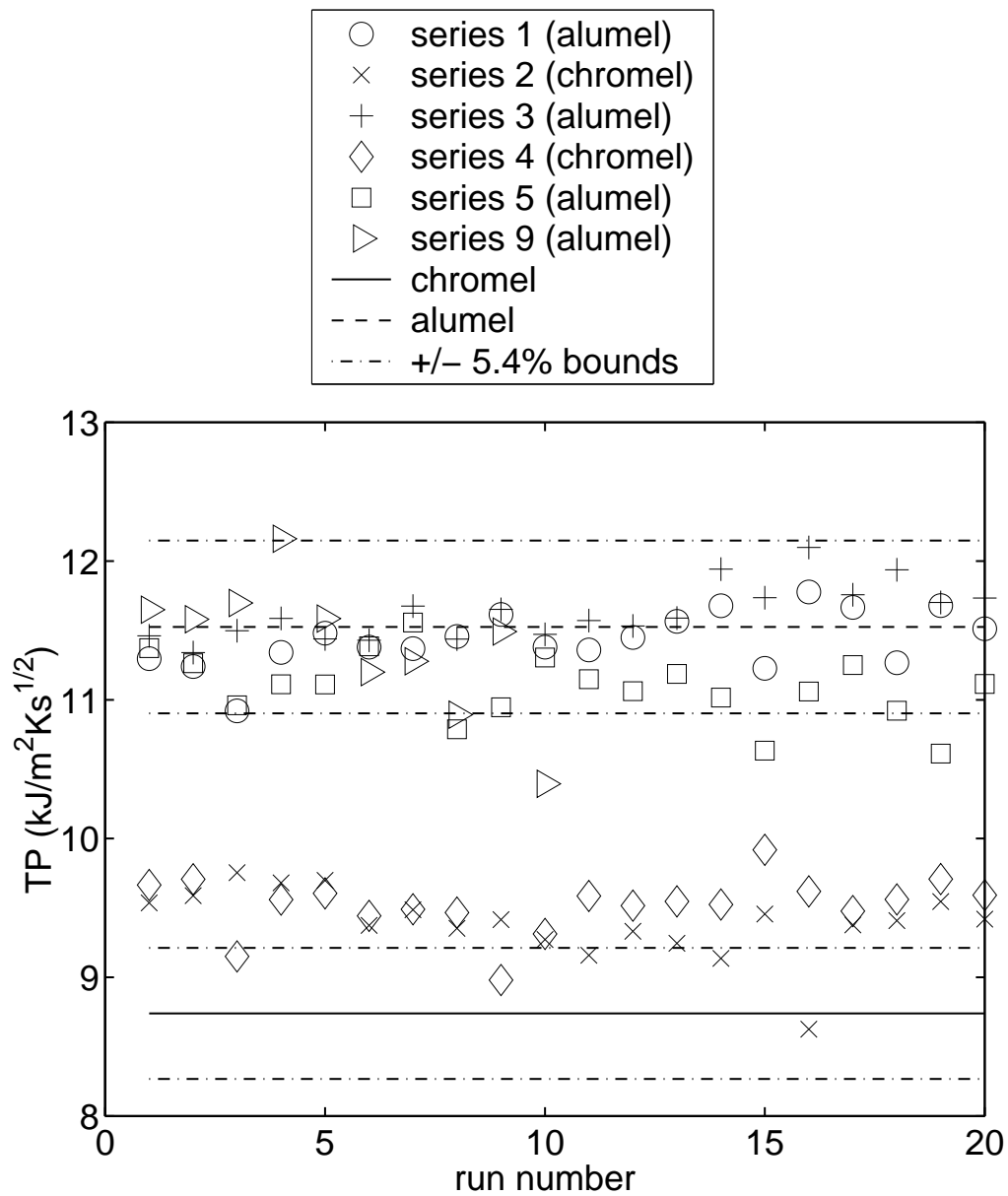


Figure 7: Results from water droplet calibration experiments for junctions created with a scalpel blade.

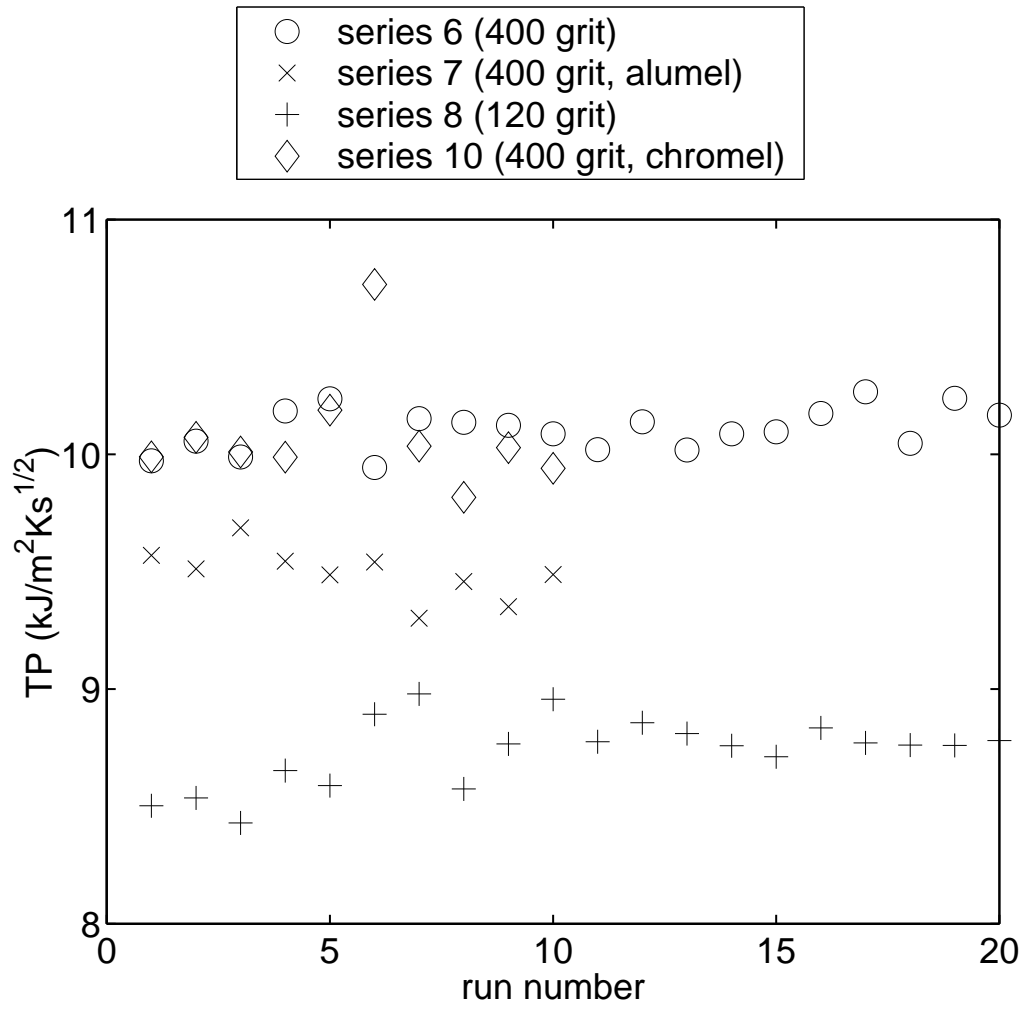


Figure 8: Results from water droplet calibration experiments for junctions created with abrasive paper.

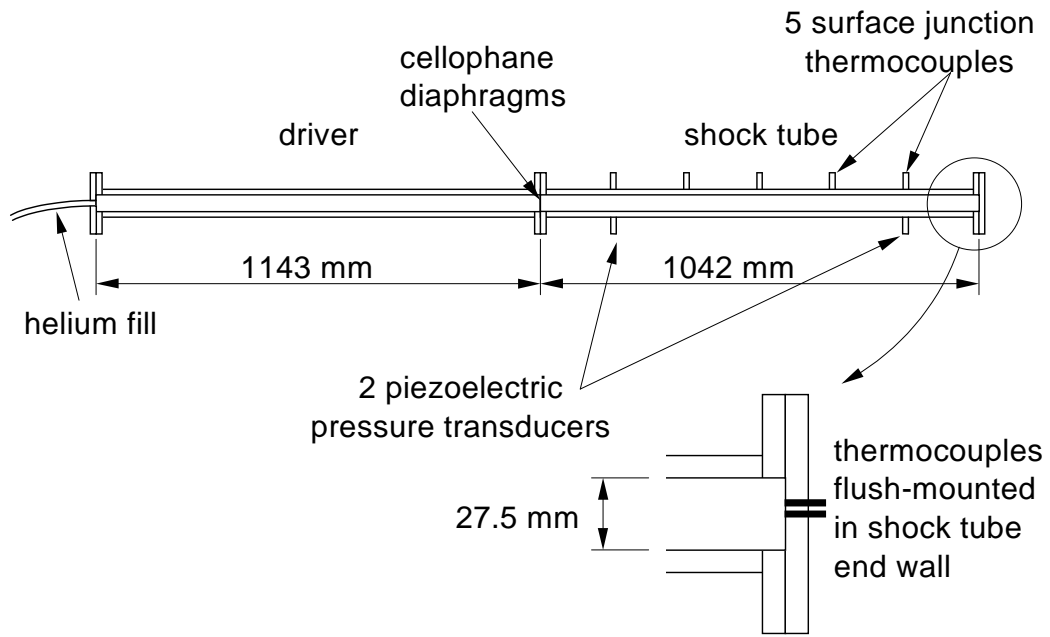


Figure 9: Illustration of the configuration used in the shock tube calibration experiments.

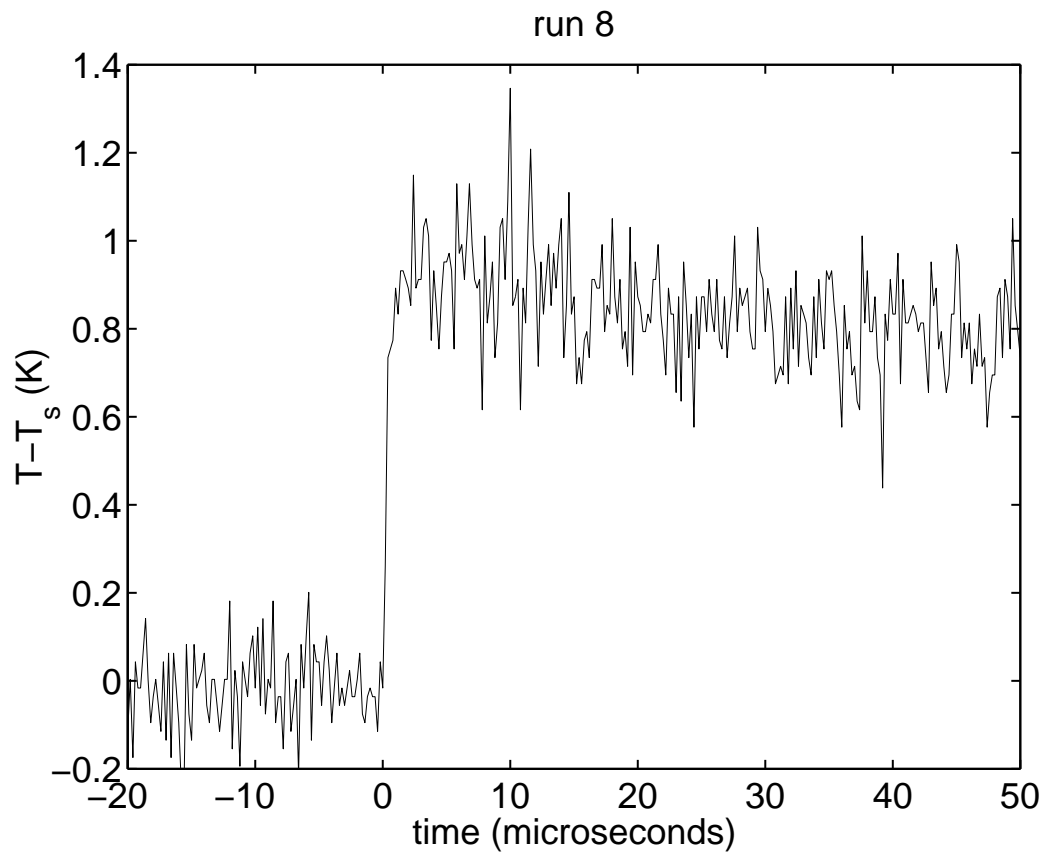


Figure 10: Example of the thermocouple temperature measured in the shock tube calibration experiments.

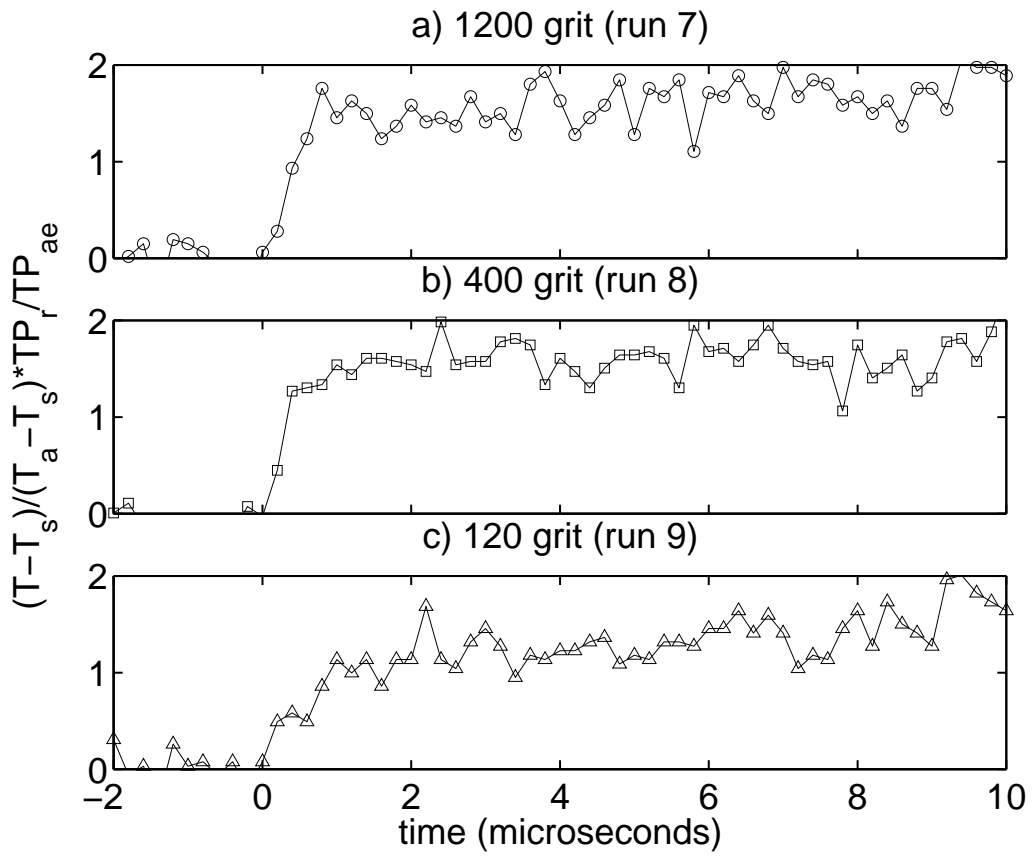


Figure 11: Results from shock tube calibration experiments: runs 7, 8, and 9 (junctions created using abrasive paper).